EFFECT OF MgO ON THE COMPOSITION AND PROPERTIES OF BELITE-BARIUM CALCIUM SULPHOALUMINATE CEMENT IN THE PRESENCE OF Na$_2$O AND K$_2$O

JIE ZHANG, #CHENCHEN GONG, LINGCHAO LU, SHOUDE WANG, PENGKUN HOU

*Shandong Provincial Key Laboratory of Preparation and Measurement of Building Materials,
University of Jinan, Jinan 250022, PR China*

#E-mail: gcc_122@sina.com

The purpose of this study is to explore the effect of MgO (1 - 9 wt. %) on the composition and properties of belite-barium calcium sulphoaluminate cement with additions of Na$_2$O and K$_2$O. The results show that 1 - 5 wt. % content of MgO can stabilize crystal types of M$_3$-C$_3$S, R-C$_3$S and β-C$_2$S. Moreover, MgO can promote the formation of C$_3$S and C$_4$AF, but has little effect on the formation of C$_{2.75}$B$_{1.25}$A$_3$\$ and C$_3$A. The C$_3$A/C$_4$AF ratio is reduced by 22 % at 5 wt. % MgO, which indicates that appropriate MgO can decrease the liquid viscosity. In the presence of Na$_2$O and K$_2$O, the highest limit of incorporated amount of MgO is about 3 wt. %, which is higher than that in Portland cement clinker of 2 wt. %. Besides, MgO favors the formation of small C$_3$S crystals in size of 4 - 20 µm. MgO enhances the hydration rate and mechanical property of cement at an optimal dosage (1 - 5 wt. %), beyond which an adverse effect could be resulted. At a MgO dosage of 5 wt. %, the compressive strengths of the cement at 1, 3, 7 and 28 days are 15.8, 39.3, 68.6 and 97.3 MPa, which increases by 116 %, 17 %, 10 % and 6 % respectively compared to the cement without MgO dopant. This study could lead to the effective use of magnesia-rich limestone in industrial production of belite-barium calcium sulphoaluminate cement.

INTRODUCTION

The Portland cement manufacture not only consumes a large quantity of raw materials and energy, but also has a considerable environmental impact [1, 2]. It takes about 1.7 tons raw materials (limestone, clay, etc.) and 8.5×10^5 kcal of energy to produce 1 ton of cement clinker, meanwhile, 0.97 tons CO$_2$ of on average are emitted per ton of cement produced, which accounts for around 6 % of all CO$_2$ anthropogenic emissions [3-7]. Considering these influences, it has been proposed that belite-rich cements are environmentally friendly cementitious materials, due to their low synthesis -temperature, low limestone consumption, low CO$_2$-emissions (less than 10 % of Portland cement), low hydration heat and good durability [4, 8-10]. However, this type of cements has low mechanical property at early ages due to the slow hydration rate of belite phase [4-6, 11, 12]. Two complementary strategies can be taken to overcome this disadvantage including the introduction of high early age strength mineral of C$_4$A$_3$\$ (also named as Klein's salt) [13-15] and the stabilization of more reactive C$_2$S (here refers to α', α, and β-C$_2$S) [16-18].

C$_{2.75}$B$_{1.25}$A$_3$\$ is a more promising mineral compared with C$_4$A$_3$\$, which is characterized by high early strength, good permeability resistance, high corrosion resistance, low alkalinity and so on [19]. In earlier research,

C$_{2.75}$B$_{1.25}$A$_3$\$ was introduced into belite-rich cement to produce belite-barium calcium sulphoaluminate cement, which is a new type of energy-efficient and environmentally friendly cement [20]. It was reported that C$_{2.75}$B$_{1.25}$A$_3$\$ enhanced the early age property of this cement compared with belite cements. However, the optimal content of C$_{2.75}$B$_{1.25}$A$_3$\$ of 9% improved the early-age strength to a limited degree [21-23]. Compared with ordinary Portland cement, it still develops relatively slow early-age property gain, which limits its industrial production and application.

In recent years, sustainable development and natural resources preservation have become global concerns. High-quality limestone resources are becoming increasingly scarce, and it is deduced that 29 billion tons will be required in the next 20 years [24, 25]. Thus, the utilization of low-grade limestone has gained much attention, and magnesia-rich limestone is one of them. It is known that magnesia-rich limestone is abundant in China[26], but due to the limitation of the MgO content in Portland cement less than 5 % by the Chinese National Standard GB175-1999, this kind of limestone' usage in Portland cement production is rare. It has been reported that for the Portland cement suitable MgO can lower the melting temperature, increase the quantity of the liquid phase [27, 28], and alter the mineral phases' crystal structure [29] and activate the reactivity of C$_3$S [30-32]. Besides,

Na_2O and K_2O (alkali), which are the most frequently existing minor components in the natural materials, have been reported to stabilize high temperature (α'_H and α) polymorphs of C_2S of belite clinkers [5, 33]. Considering the advantages of introducing foreign dopants into belite cements, improvements of the properties of belite-barium calcium sulphoaluminate cement with MgO, Na_2O and K_2O to save the high-grade limestone resources and release the environmental burden would be expected, however, to the current authors' knowledge no such work has been reported.

This study investigates the role of MgO in the minerals' formation of belite-barium calcium sulphoaluminate cement clinker and the hydration and hardening properties such as compressive strength development, hydration rate, hydration heat release and microstructures of hydration products in the presence of Na_2O and K_2O by using chemical reagents. It is hoped that this paper could offer available data for further industrial production of belite-barium calcium sulphoaluminate cement and effective utilization of magnesia-rich limestone in this type of cement clinker.

EXPERIMENTAL

Sample preparation

The cement clinker was synthesized using analytical reagent grades of $CaCO_3$, SiO_2 (99.0 % from Damao Chemical Reagent Factory, China), Fe_2O_3, Al_2O_3, $BaSO_4$, $BaCO_3$, CaF_2, MgO, Na_2CO_3 and K_2CO_3 (99.0 % from Sinopharm Chemical Reagent Co., Ltd, China), to eliminate the influences of other impurities as much as possible. The designed mineral composition and chemical composition of belite-barium calcium sulphoaluminate cement clinker are listed in Table 1 (the blank clinker without dopants), and 0.6 % CaF_2 was added as the mineralizing agent. For the reference sample, 0.2 wt. % Na_2O and 0.5 wt. % K_2O ($Na_2O·eq =$ $= 0.529$; percentage in relation to the blank clinker, the same as follows) were added into the raw materials of belite-barium calcium sulphoaluminate cement clinker. Then five doped samples were prepared by adding 1, 3, 5, 7 and 9 wt. % MgO into the reference.

Raw materials (finer than 74 μm) were mixed and wet ground in the planetary mill for 40 minutes to ensure a homogenous blend. Mixtures were then dried to a water content of about 10 % and compressed to form $\varnothing$ 60 × 10 mm cylinders. The cylinders were oven-dried at 105°C for 1-2 h before being calcined at a heating rate of 5°C·min^{-1} to 1380°C and held for 90 min and then

cooled immediately. The calcined samples were ground to the residue weight of a 74 μm sieve less than 5 % by a planetary mill prior to property determinations.

The ground clinkers were mixed with 10.0 wt. % $CaSO_4·2H_2O$ (99.0 % from Sinopharm Chemical Reagent Co., Ltd, China). Pastes were prepared at a water/cement ratio of 0.30, cast in 20 mm × 20 mm × 20 mm molds, vibrated to remove air bubbles, and then wiped the surface flat with the scraper. The molded pastes were kept at 20 ± 2°C and relative humidity exceeding 95 % for 24 h, and then removed from the molds. The demolded samples were cured in a water tank at 20 ± 2°C for 3, 7 and 28 days.

Characterization

Free-CaO tests

The content of free-CaO in cement clinkers was measured according to ethanediol-alcohol method by the fast f-CaO measurement apparatus.

X-ray diffraction (XRD)

XRD data were collected on D8 ADVANCE X-ray diffractometer with strictly monochromatic Cu Kα radiation ($\lambda = 0.154$ nm) produced by Bruker in Germany. The overall measurements for clinkers were carried out in the range of 10° to 60° (2θ) with a step size of 0.02° (2θ), a step time of 4 s per pattern, an accelerating voltage of 40 kV and a current of 40 mA. Besides, the measurements for hydration products were carried out in the range of 5° to 60° (2θ) with a step size of 0.02° (2θ), a step time of 0.2 s per pattern.

To quantitatively evaluate the amount of crystalline phases in the samples, Quantitative XRD (Q-XRD) technique was used during this work. Q-XRD results were obtained through the Rietveld method [34, 35]. All the samples were characterized by Laboratory X-ray powder diffraction (LXPRD). LXPRD plots were analyzed by using the Rietveld method with Topas 4.2 software package [36-38] from Bruker AXS GmbH.

Petrographic description

Microscopic images of clinkers were captured by using a Motic 310A microscope (Motic Instruments Inc., Canada) equipped with a Moticam Pro 285A camera. The samples were embedded in the sublimed sulfur before polishing. The polishing process was performed on the glass by hand with three kinds of fineness of aluminium

Table 1. Designed mineral composition (wt. %) and chemical composition of raw materials (expressed as oxides, wt. %).

C_3S	C_2S	C_3A	C_4AF	$C_{2.75}B_{1.25}A_3\$$	SiO_2	Al_2O_3	Fe_2O_3	CaO	SO_3	BaO
37.5	37.5	4.6	11.5	9.0	22.4	7.7	3.7	60.6	1.4	4.1

oxide, and the polished samples were cleaned in absolute ethyl alcohol with an ultrasonic cleaner for 10 minutes. The polished surface was etched in 1 % ammonium chloride aqueous solution for 6 seconds.

Scanning electron microscopy (SEM)

Pieces of hydrated samples at different ages were coated with carbon to provide a conductive surface for SEM imaging. Observation of mineral morphological feature was examined by using a Field Emission Scanning Electron Microscope (GUANTA 250-FEG, USA) with a Link Energy Disperse Spectroscopy (LinkISIS300 type, USA) system. The distribution of elements in minerals was analyzed by Energy Spectrum analysis (EDS).

Compressive strength test

Compressive strength tests were carried out by an universal compression machine (MTS CMT5504, USA). The determination of compressive strength was performed after 1, 3, 7 and 28 days of hydration, and subsequently the hydration reactions of the cement pastes were stopped by absolute ethyl alcohol. Each resultant value of compressive strength was an average calculated from six determinations.

Hydration heat-evolution test

An isothermal heat-conduction calorimetry (TAM air C80, Thermometric, Sweden) was used to measure the hydration heat evolution of clinkers mixed with 10.0 wt. % $CaSO_4 \cdot 2H_2O$. The water/cement ratio was 0.3 and experimental temperature was $30.0 \pm 0.1°C$. Cements and water were tempered for several hours before mixing, then the water was injected into the reaction vessel and the samples were stirred in the calorimeter for several minutes. This procedure allowed monitoring the heat evolution from the very beginning when water was added to samples. Data acquisition was performed for about 6 days.
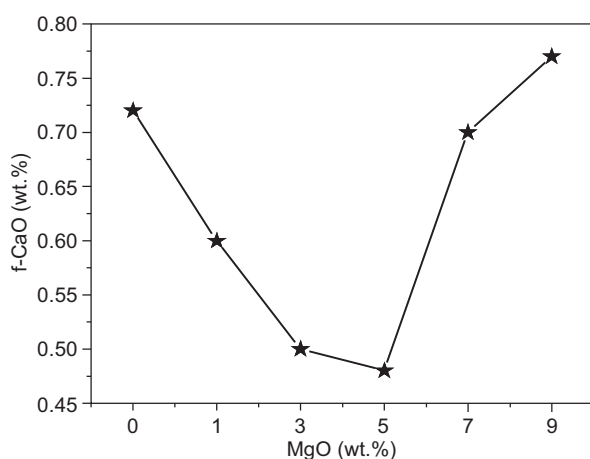
RESULTS AND DISCUSSION

The effect of MgO on mineral phase formation of cement clinker

Burnability

Content variations of f-CaO in clinker samples with the addition of MgO are given in Figure 1. The low content of f-CaO (less than 0.8 wt. %) in all samples is a good indicator of the burnability of the raw meal. It can be seen that the content of f-CaO decreases firstly and then increases as the amount of MgO rises. When the dosage of MgO is 0 - 3 wt. %, the decrease in f-CaO content is more remarkable, and it reaches the lowest point as little as 0.48 wt. % at 5 wt. % MgO. This is attributed to good fluxing effect of MgO, because a suitable amount of MgO can decrease the viscosity of liquid phase and increase the content of liquid phase to promote the formation of C_3S, during which f-CaO is consumed [39, 40]. However, the f-CaO content increases remarkably when MgO dosage is over 5 wt. %. This incidates that a high MgO content (> 5 wt. %) is not helpful for the burnability.

Mineral composition

XRD patterns of all studied clinkers are shown in Figure 2. The quantitative phase analysis of clinker minerals in different polymorphs will be discussed below. It can be seen from Figure 2 that characteristic mineral $C_{2.75}B_{1.25}A_3\$$ and the main minerals of Portland cement are seen in this new type of cement clinker. The characteristic diffraction peaks of $C_{2.75}B_{1.25}A_3\$$ vary little with increasing MgO content, indicating that MgO
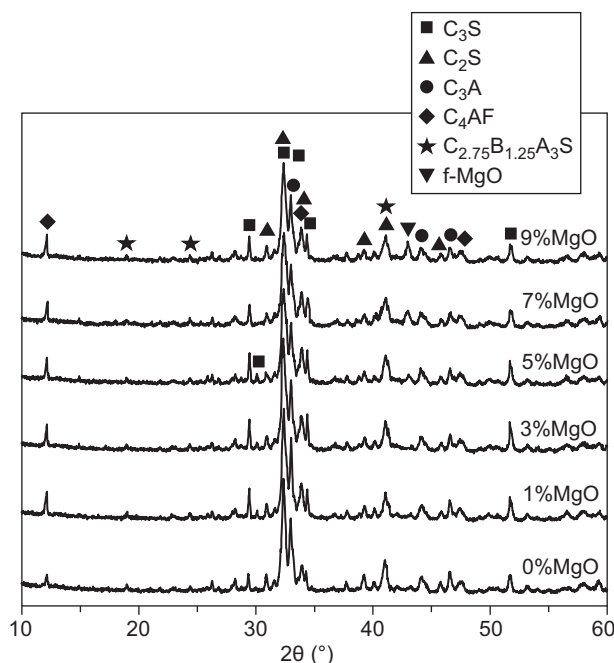
Figure 1. f-CaO content of clinker samples.

Figure 2. XRD patterns of cement clinkers doped with MgO, Na₂O and K₂O.

has little effect on the formation of $C_{2.75}B_{1.25}A_3\$$. Besides, when the dosage of MgO reaches 5 wt. %, the diffraction peak of f-MgO at about 42° (2θ) appears and its intensity increases with the MgO content increasing, which indicates that excess MgO in the clinker will result in f-MgO (periclase).

As shown in Figure 2, the diffraction peaks of C_2S, including the overlapping peak (2θ = 32.9°) and the unshielded peak (2θ = 30.9°) decrease with the increase of MgO. Whereas, the intensities of non-overlapping peaks of C_3S, at about 29°, 34° and 52° (2θ), respectively, obviously increase with adding 1 - 5 wt. % MgO, but they are weakened when MgO dosage is over 5 wt. %. Besides, it is noted that one C_3S peak (2θ = 30.1°) appears at 1 - 5 wt. % MgO. This means that 1-5 wt. % MgO promotes the formation of C_3S, in agreement with its effect on C_3S formation in Portland cement clinker [41-43]. In addition, the intensity of C_4AF peak (2θ = = 12.1°) increases with the addition of MgO while the C_3A peaks vary little. This variation suggests that MgO promotes the formation of C_4AF, which is consistent with Li's findings [26, 43], but affects little on the formation of C_3A.

Rietveld quantitative phase analysis

There are various crystalline phases in belite-barium calcium sulphoaluminate cement clinker, and some crystalline phase displays polymorphism. During the Q-XRD analysis, $C_{2.75}B_{1.25}A_3\$$ mineral was not taken into account as its crystal structure data for Rietveld quantitative analysis has not been established, and the doping elements has little effect on its formation as discussed above. Table 2 shows the quantitative phase analysis results for all clinkers, as well as the Rietveld agreement factor for the refinements. It was observed that f-MgO generates when the MgO dosage exceeds 5 wt. %, corresponding to the results shown in Figure 2. For belite-barium calcium sulphoaluminate cement clinker, the highest limit of incorporated amount of MgO is about 3 wt. %, which is higher than that of Portland cement clinker of 2 wt. % [26, 40, 43]. This may be attributed to the existence of SO_3 in the cement clinker that contributes to the diffusion of MgO in the liquid phases [44].

Silicate phases

Figure 3 shows the relative content of high temperature polymorphs (M_3 and R) of C_3S, which is calculated from quantitative phase analysis. In the clinkers, T_3-C_3S, M_3-C_3S and R-C_3S are all detected; it has been reported that M_3-C_3S and R-C_3S perform better hydration activity than T_3-C_3S [45]. From Figure 3, it can be seen that the addition of MgO influences the ratio of polymorph forms for C_3S. T_3-C_3S is significantly reduced and more M_3-C_3S and R-C_3S are stabilized, which may contribute to the increase of the compressive strength. When MgO dosage is 1 - 5 wt. %, M_3-C_3S and R-C_3S content are higher, meanwhile, the total content of C_3S can be up to 35.63 - 38.20 wt. % (Table. 2). However, great decrease of C_3S and R-C_3S are seen at 7 wt. % which corresponds well with the results as shown in Figure 1. Thus, it can be concluded that 1 - 5 wt. % MgO favors the formation of C_3S and the stabilization of M_3-C_3S and R-C_3S. The Mg ions exclusively replacing the Ca-sites in the structure of C_3S are thus essential to the presence of R and M_3 [46].
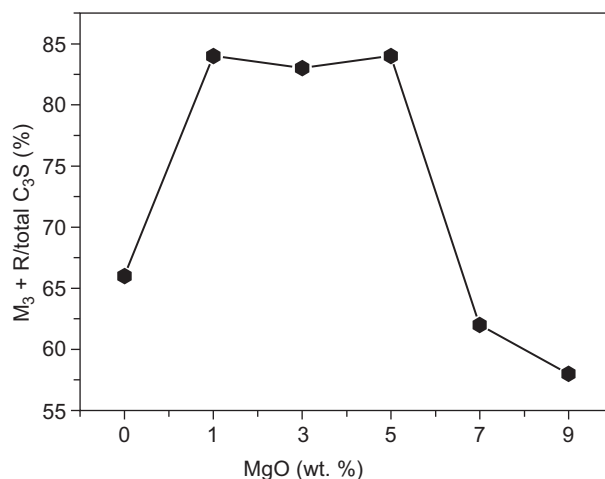

Figure 3. Relative content of M_3-C_3S and R-C_3S in samples.

The content of belite phase crystallized in different polymorphs present in clinkers co-doped with MgO calculated from quantitative phase analysis is illustrated in Figure 4. It has been reported that the order of

Table 2. Rietveld quantitative phase analysis results of mineral composition of the resultant clinkers (wt. %).

Lables	Na$_2$O dosage	K$_2$O dosage	MgO dosage	C$_3$S	C$_2$S	C$_3$A	C$_4$AF	f-CaO	f-MgO	Rwp*
M0	0.2	0.5	0	34.59	48.03	6.83	9.83	0.72	0.00	14.25
M1	0.2	0.5	1	35.63	43.04	7.65	13.08	0.60	0.00	11.87
M3	0.2	0.5	3	38.20	44.82	5.54	10.94	0.50	0.00	12.19
M5	0.2	0.5	5	36.80	42.89	5.72	12.08	0.48	1.83	13.68
M7	0.2	0.5	7	30.22	41.96	9.79	13.16	0.70	4.17	12.09
M9	0.2	0.5	9	32.63	39.09	9.36	12.17	0.77	5.98	13.75

* Rwp is the agreement factor of the Rietveld refinement

hydration degree for different types of C_2S is α-C_2S > α'_H-C_2S > β-C_2S > α'_L-C_2S > γ-C_2S during the same curing period and condition, and γ-C_2S scarcely reacts with water at ambient temperature [47-49], so γ-C_2S is not the desirable polymorph. In the present study, it can be seen from Figure 4 that different amount of β-C_2S and α'_L-C_2S exist and no γ-C_2S is found. The content of α'_L-C_2S decreases on different levels and more β-C_2S is formed in MgO-doped samples. The total content of C_2S decreases when MgO is added. It can be concluded that MgO typically favors the formation of β- C_2S in the presence of Na₂O, K₂O.
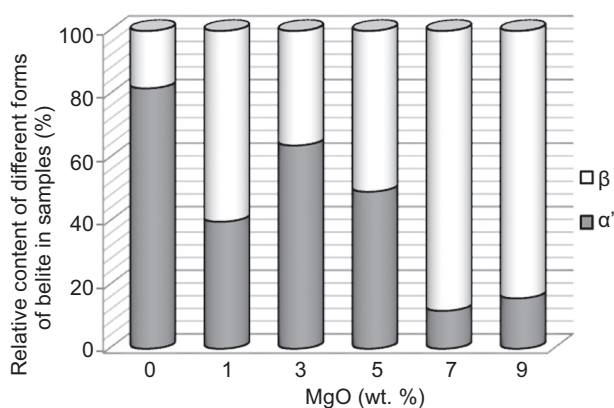

Figure 4. Content of different polyforms of belite in cement clinkers.

Interstitial phases

In belite-$C_{2.75}B_{1.25}A_3$\$ cement clinker, C_3A, C_4AF and $C_{2.75}B_{1.25}A_3$\$ all belong to the interstitial phases [20]. According to the results of Figure 2, C_3A and C_4AF are further studied here. It has been reported that MgO dominates the C_3A formation and the increase of MgO can decrease the amount of C_3A in Portland cement [26], however this rule was not observed in this study and the formation of C_3A is not regular with different doping amounts of MgO (Table 2). It has to be highlighted that
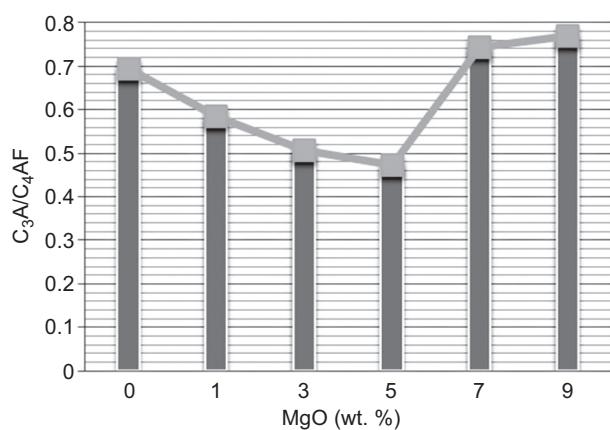

Figure 5. The variation curve of C_3A/C_4AF ratio of the resultant clinkers.

the liquid viscosity is significantly influenced by the dopants. The liquid viscosity is characterized by the C_3A/C_4AF ratio of the clinkers. The results are illustrated in Figure 5. It can be seen that the C_3A/C_4AF ratio shows a tendency of decrease and then increase in the clinker samples along with MgO dosage increasing. The C_3A/C_4AF ratio decreases when the MgO dosage is lower than 7 wt. % and the minimum is 0.47 when the dosage of MgO is 5 wt. %. This indicates that appropriate MgO is in favour of decreasing the liquid viscosity, and in the presence of Na₂O and K₂O, more MgO up to 5 wt. % is better for the clinkers' sintering. The results are in accordance with the results of Figure 1.

Microscopic observation

The microscopic images of clinkers captured by metallurgical microscope are displayed in Figure 6. It is known that in cement clinker alite occurs as an-gular subhedral to euhedral crystals in blue color, whereas belite occurs as round and lamellar crystals in tan-to-brown color [43, 50]. In the reference sample, alite and belite are in the size of 8 - 30 μm and 5 - 40 μm, respectively. The smaller dimension of alite compared to that in OPC cement clinker is attributed to the lower synthesis temperature. It can be seen from Figure 6 that the matrix of dark aluminate (C_3A) and brightly reflecting ferrite phase (C_4AF) and barium-bearing calcium sulfoaluminate ($C_{2.75}B_{1.25}A_3$\$) are among the C_3S and C_2S crystals. With MgO doping, smaller alite crystals in size of 4 - 20 μm form but belite crystals vary little in size. Besides, some small particles, maybe f-MgO, distributed in the interstitial phases are observed in the sample with 5 wt. % MgO, which may increase the viscosity of the liquid phase and block the consumption of f-CaO, and this is in line with the results of Figure 1 and Figure 2. F-MgO in the clinkers may do little harm to the soundness of cement due to their small size (3 - 8 μm) and the lower sintering temperature [51]. In M0, M3 and M5 clinkers, the minerals show a homogeneous distribution, and the texture on belite crystals is obvious, which will be beneficial to the strength development. However, in M7 clinker, the rims of alite and belite all become unsmooth and it shows poorer crystallization, moreover, some wrappage appears in alite and belite, which may affect the hydration.

Table 3. Strength increase rate of MgO-doped samples relative to the reference sample (M0).

Sample label	Strength improvement rate (versus M0, %)			
	1 day	3 days	7 days	28days
M1	14	13	8	6
M3	103	12	5	7
M5	116	17	10	6
M7	140	-13	-23	-24
M9	75	-19	-17	-14

a) M0
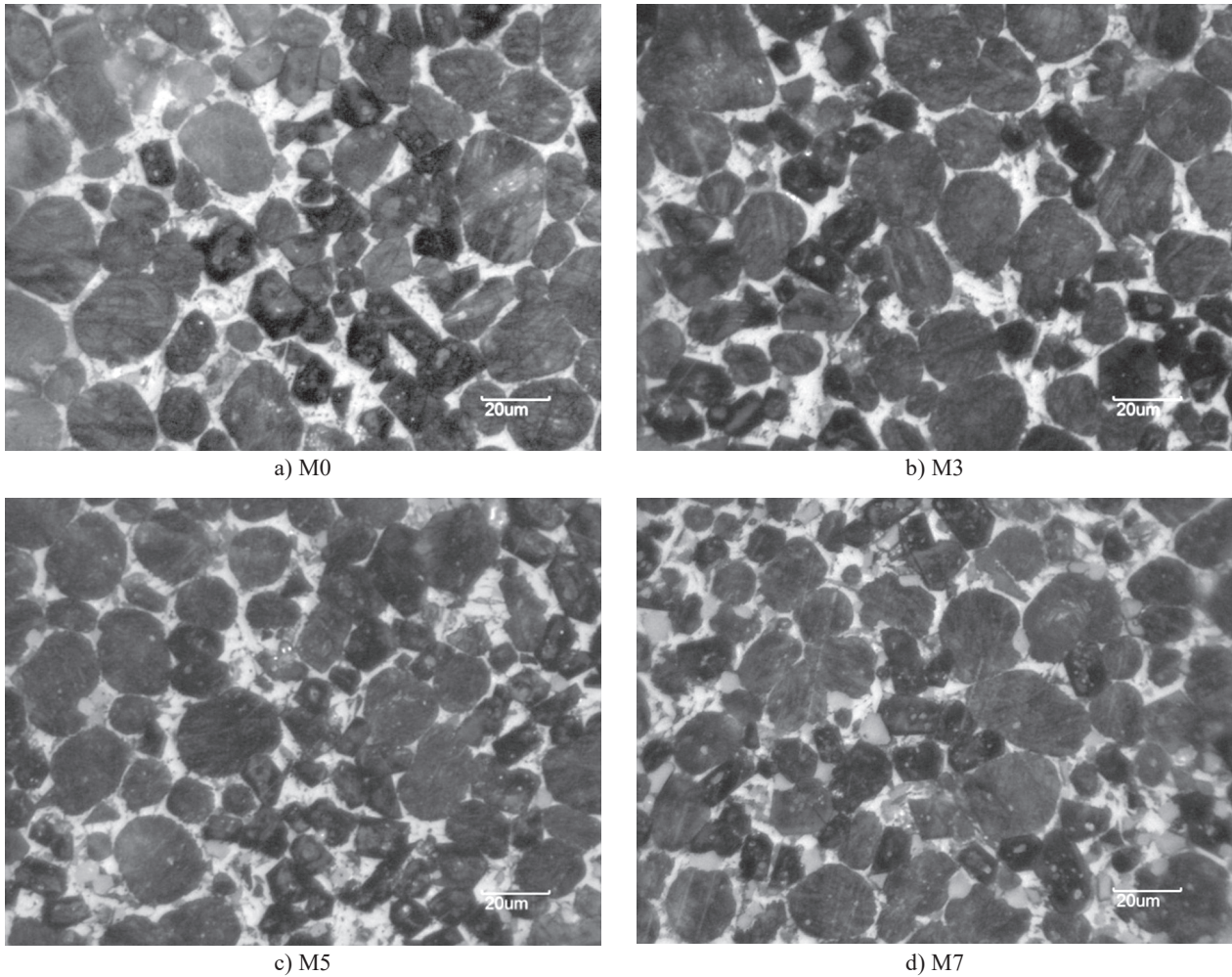

b) M3

c) M5

d) M7

Figure 6. Microscopic view of clinker samples.

The effect of MgO on hydration properties of cement

Compressive strength

Compressive strength of samples doped with MgO, Na_2O and K_2O are shown in Figure 7. The dash dot lines were drawn based on the strength of the reference sample at the desired ages. Table 3 gives the strength increase rate of samples doped with MgO. Based on the results, at 1 day, the strengths of M3, M5 and M7 are higher, which are increased by over 100 % compared to the reference (Table 3). However, M7 cement paste develops low strength as the extension of curing ages, whose strength is just 69.3 MPa at 28 days. Similarly, the strength of M9 sample has the same variation trend. In contrast, the performance of M1, M3 and M5 are comparable at 3 days, 7 days and 28 days, and generally superior to that of the reference cement (M0). The strength of M5 sample after 7 days is 68.6 MPa, increased by 10 % in comparison with the reference, and only 0.7 MPa smaller than that of M7 at 28 days. This is owing to the improved C_3S and C_2S polymorphs and the more content of C_3S in M1, M3 and M5 samples. These characteristics lead to

the improvement of the hydraulic properties. It thus can conclude that an appropriate amount of MgO (1 - 5 wt. %) increases the compressive strength but excess MgO inevitably decreases the strength. This corresponds well to the results discussed above.
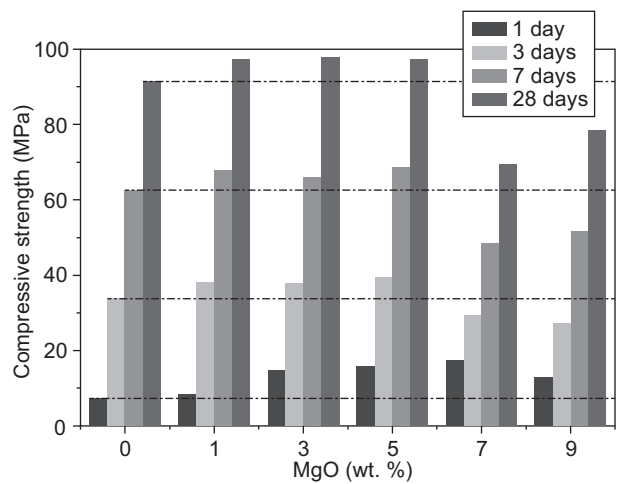

Figure 7. Compressive strengths of cement pastes.

XRD patterns of hydration products

The unhydrated silicates and hydration products of CH and AFt are examined by X-ray diffraction shown in Figure 8. Although the diffraction peak intensity is not linearly proportional to the content of crystalline phases, some important information can be obtained from the comparisons of the relative intensity and changes of the intensity with the prolongation of hydration ages. As shown in Figure 8, CH peaks at 18.0° (2θ) of hydrating cement with 1 wt. %, 3 wt. % and 5 wt. % MgO (M1, M3 and M5) are higher than others' at 3 days (Figure 8a). It means that 1 - 5 wt. % MgO promotes the hydration of cement samples, but 7 - 9 wt. % MgO has an obvious delaying effect. At the same time, the variation in peak of

AFt at 9.0° reflects the same results. At 28 days, a similar trend appears and the intensities of CH and AFt peaks obviously increase compared to those at 3 days, and accordingly the intensities of peaks of silicates obviously decrease.

Hydration heat

To reflect the effect of MgO on the hydration of cement in detail, the heat liberation of hydration of M0, M5 and M7 during 140h are further measured as shown in Figure 9. Figure 9a and Figure 9b respectively displays the rate of hydration heat released and the cumulative heat release. Rather intense heat liberation within few hours is due to the initial rapid hydration of C_3A and
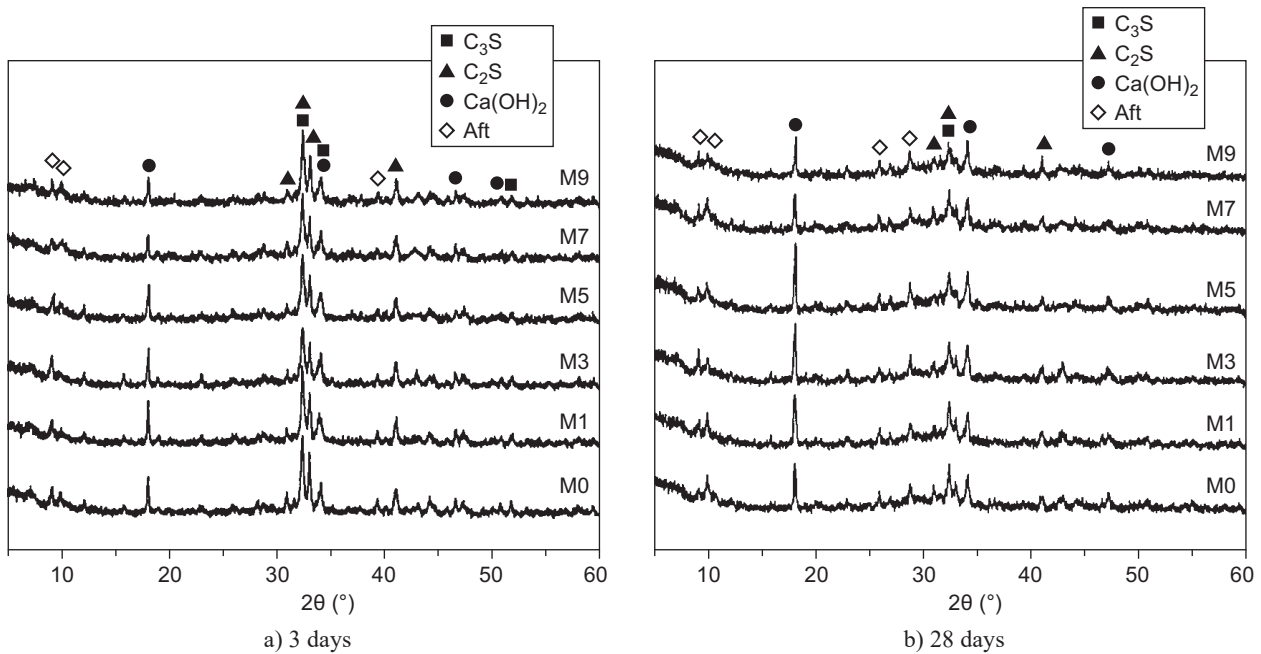

a) 3 days

b) 28 days

Figure 8. XRD patterns of studied pastes hydrated at the curing ages: a) 3 days; b) 28 days.
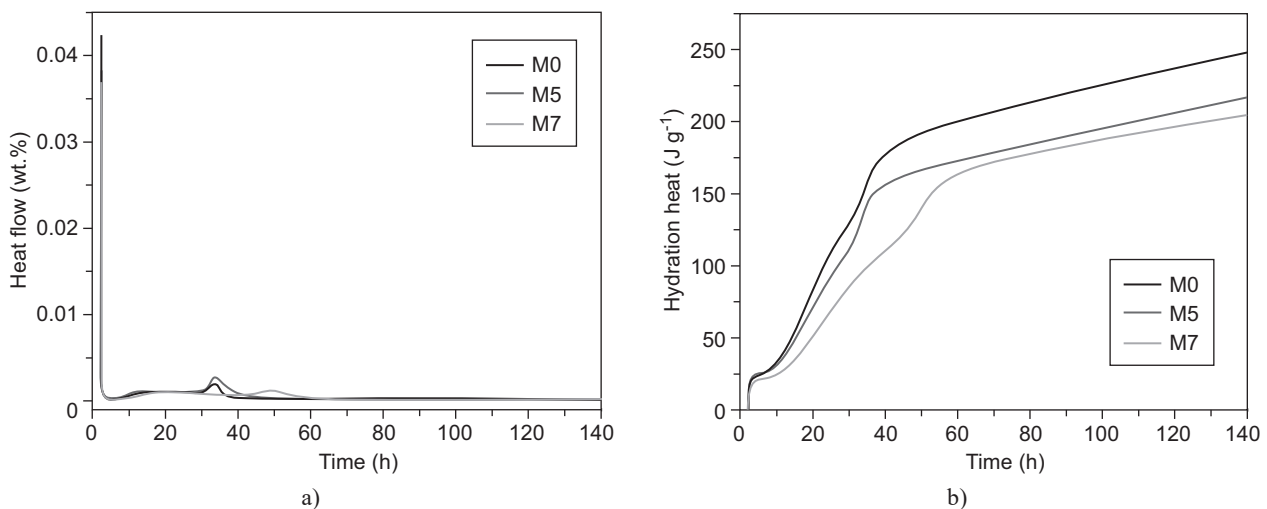

a)

b)

Figure 9. Calorimetic heat flow and heat curves for the studied samples (M0, M5 and M7).

$C_{2.75}B_{1.25}A_3\$$ in the pre-induction period [52, 53]. Soon thereafter, the overall rate of hydration is slowed down in the induction period and then a second main exothermic peak appears which is mainly due to the hydration of C_3S (Figure 9a). The end time of the induction period has an important effect on cement hydration. It can be seen that the induction period of M7 is nearly 15 hours longer than those of M0 and M5, moreover, hydration rate in

M5 is the highest. The overall heat evolved for M0, M5 and M7 samples for 140 h are 219, 250 and 206 J·g^{-1}, respectively, which also indicates that M5 hydrates fastest but M7 hydrates slower than the reference. This is in accordance with the results of compressive strength development trend.

Microstructures of hydration samples

Figure 10 displays the SEM and EDS photographs of the fracture surface of hardened pastes at 3 days. As shown in Figure 10, the main hydration products after 3 days are needle-like ettringite, large crystal hexagon plates of CH crystals and the cotton-shaped structure of C–S–H. Ettringite is mainly in the form of Ba-bearing ettringite (Figure 10a, b). In the reference sample, short acicular ettringite, large overlapped CH and small amount of C–S–H are observed; meanwhile, there exists some cracks (Figure 10a). However, more long acicular ettringite and C–S–H pahses in M5 are observed, and compacter microstructures are observed in both images of M5. From Figure 10c, except for the same hydrated products, unhydrated minerals, cracks and black pores are obviously observed, which shows a relatively looser microstructure. Thus, the compactness and less cracks of the hydrated M5 pastes support the increased strength of the cement pastes.

CONCLUSIONS

From the present study, the following major conclusions can be drawn:

- Appropriate amount of MgO (1 - 5 wt. %) can improve the burnability of raw materials, promote the formation of C_3S, and stabilize M_3-C_3S and R-C_3S. In addition, MgO favors the formation of small C_3S crystals in size of 4 - 20 μm.

- MgO favors the formation of β-C_2S. Excessive MgO (> 5wt. %) decreases the amount of C_2S.

- MgO favors the formation of C_4AF, but affects little on the formation of $C_{2.75}B_{1.25}A_3\$$ and C_3A. 5 wt. % MgO reduces the C_3A/C_4AF ratio by 22 %, but 7 wt. % MgO makes it increased by 11 %. This indicates that appropriate MgO decreases the liquid viscosity but an excessive MgO will have adverse side effects.

- 1 - 5 wt. % MgO can increase the compressive strength of the cement, but excessive MgO will lead to negative effect. The compressive strength of the sample with 5 wt. % MgO at 1, 3, 7 and 28 days are 15.8, 39.3, 68.6 and 97.3 MPa, which increases by 116 %, 17 %, 10 % and 6 % respectively compared to the cement without MgO dopant.

- MgO (1 - 5 wt. %) promotes the hydration rate but more MgO delays the hydration process. CH and AFt obviously increase according to XRD patterns.
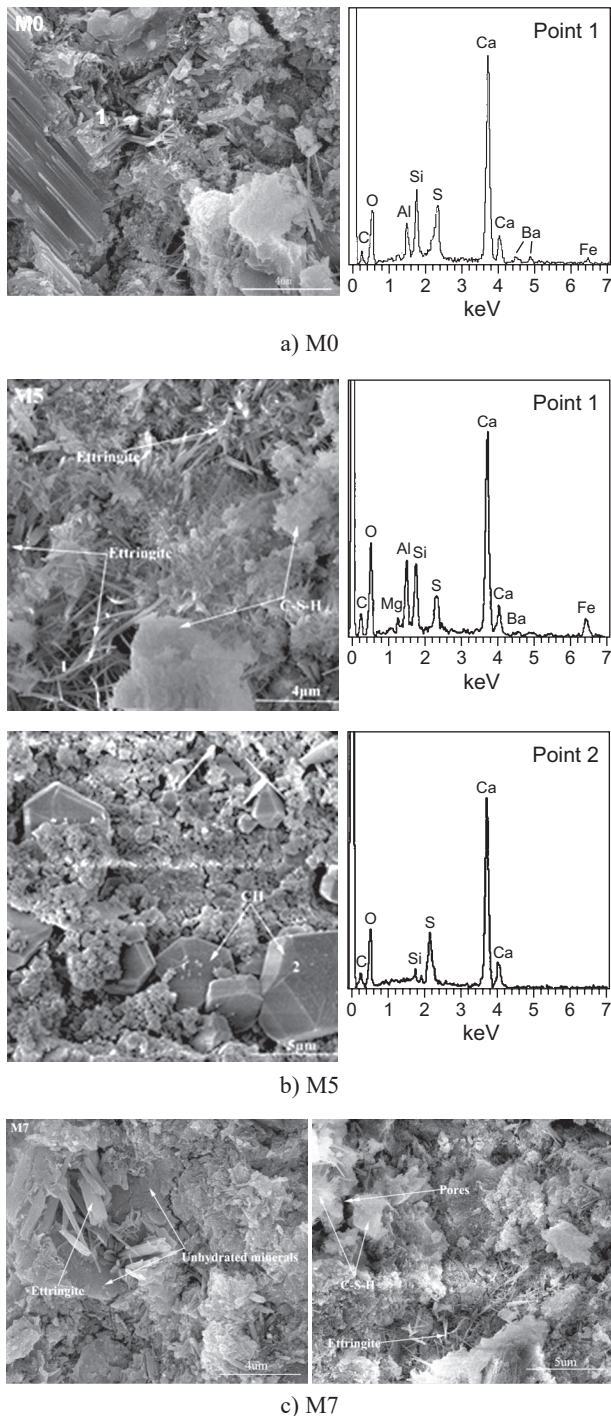

Figure 10. SEM-EDS images of hydrated cement pastes at 3 days; a) M0: the reference; b) M5: samples doped with 5 wt. % MgO; c) M7: samples doped with 7 wt. % MgO.

The hydration rate of sample with 5 wt. % MgO in acceleration period is 0.84 mW·g^{-1} higher than that of the reference sample, but 7 wt. % MgO enlongs the induction period for about 15 hours compared to that of the reference.

● Sample with 5 wt. % MgO displays a dense and compact microstructure, in which more long acicular ettringite and C–S–H phases are observed.

● In belite-barium calcium sulphoaluminate cement clinker doped with Na$_2$O and K$_2$O, the highest limit of incorporated amount of MgO is about 3 wt. %, which is higher than that in Portland cement clinker of 2 wt. %.

It can be deduced that an appropriate amount of MgO is favorable for the optimization of the mineral composition and properties of belite-barium calcium sulphoaluminate cement. In the presence of Na$_2$O and K$_2$O, MgO as high as 5 wt. % can be introduced into the cement clinker, makeing it promising for the industrial production of belite-barium calcium sulphoaluminate cement. From this study, it demonstrates the potential of utilizing low-grade magnesia-rich limestone to make the cementitious materials greener, stronger and more economical.

REFERENCES

1. Arjunan P., Silsbee M.R., Roy D.M.: Cem. Concr. Res. *29*, 1305 (1999).
2. Puertas F., Garcia I.D., Barba A., Gazulla M.F., Palacios M., Gomez M.P., Ramirez S.M.: Cem. Concr. Res. *30*, 798 (2008).
3. Gartner E.: Cem. Concr. Res. *34*, 1489 (2004).
4. De la Torre AG., Aranda M.A.G., De Aza A.H., Pena P., De Aza S.: Bol. Soc. Esp. Ceram. Vidrio. *44*, 185 (2005).
5. Morsli K., De la Torre A.G., Zahir M., Aranda M.A.G.: Cem. Concr. Res. *37*, 639 (2007).
6. Morsli K., De la Torre A.G., Stöber S., Antonio J.M.C.,Zahir M., Aranda M.A.G.: J. Am. Ceram. Soc. *90*, 3205 (2007).
7. IAcobescu R.I., Koumpouri D., Pontike Y., Angelopoulos G.N.: Ceramics – Silikáty *57, 126* (2013)
8. Chatterjee A.K.: Cem. Concr. Res. *26*, 1213 (1996).
9. Kacimi L., Masseron A.S., Salem S., Ghomari A., Derriche Z.: Cem. Concr. Res. *39*, 559 (2009).
10. Kim Y.M., Hong S.H.: J. Am. Ceram. Soc. *87*, 900 (2004).
11. Cuberos A.J.M., De la Torre A.G., Pinazo G.A., Sedeno M.C.M., Schollbach K., Pollmann H., Aranda M.G.: Environ. Sci. Technol. *44*, 6855 (2010)
12. Popescu C.D., Muntean M., Sharp J.H.: Cem. Concr. Comp. *25*, 689 (2003).
13. Glasser F.P., Zhang L.: Cem. Concr. Res. *31*, 1881 (2001).
14. Zhang L., Su M.Z., Wang Y.M.: Adv. Cem. Res. *11*, 15 (1999).
15. Ma B., Li X.R., Mao Y.Y., Shen X.D.: Ceramics-Silikáty *57*, 7 (2013).
16. Stark J., Muller A., Seydel R., Jost K. in: Proceedings of the 8th International Congress of Cement Chemistry, p. 306-309, Rio de Janeiro, Brazil, 1986.
17. Gies A., Knofel D.: Cem. Concr. Res. *16*, 411 (1986).
18. Morsli K., De la Torre A.G., Stöber S., Cuberos A.J.M., Zahir M., Aranda M.A.G.: J. Am. Ceram. Soc. *90*, 3205 (2007).
19. Wang S.D., Huang Y.B., Gong C.C., Lu L.C., Cheng X.: Adv. Cem. Res. *26*, 169 (2013).
20. Lu L.C., Zhang W.W., Ye Z.M.: ZL 200610045503.6, Chinese Patent, 2007.
21. Zhang W.W., Lu L.C., Chang J.: J. Chin. Ceram. Soc. *26*, 345 (2007).
22. Zhang W.W., Lu L.C., Cui Y.J.: J. Chin. Ceram. Soc. *35*, 467 (2007).
23. Lu L.C., Zhang W.W., Xuan Z.H.: J. Chin. Ceram. Soc. *36*, 166 (2008).
24. Gineys N., Aouad G., Sorrentino F., Damidot D.: Cem. Concr. Res. *41*, 1177 (2011).
25. Qiu G.H.: *Experimental research on utilization of coal gangue, tailings as clay mixed with low-grade limestone for cement clinker calcinations*, M.S. Thesis, Zhejiang University, 2012.
26. Li X.R., Huang H., Xu J., Ma S.H., Shen X.D.: Constr. Build. Mater. *37*, 548 (2012).
27. Taylor H.F.W.: Acdemic Presee, p.48-50, London, 1997.
28. Altun A.I.: Cem. Concr. Res. *29*, 1867 (1999)**.**
29. De la Torre A.G., De Vera R.N., Cuberos A.J.M., Aranda M.A.G..: Cem. Concr. Res. *38*, 1261 (2008).
30. Stephan D., Dikoundou S.N., Sieber R.G..: Thermochim. Acta. *672*, 66 (2008).
31. Parkash R.: Cem. Concr. Res. *28*, 867 (1998).
32. Stephan D., Wistuba S.: J. Eur. Ceram. Soc. *26*, 161 (2006).
33. Gies A., Knofel D.: Cem. Concr. Res. *16*, 411 (1986).
34. Rietveld H.M.: J. Appl. Crystallogr. *2*, 65 (1969).
35. De la Torre A.G., Aranda M.A.G.: J. Appl. Crystallogr. *36*, 1169 (2003).
36. Cheary R.W., Coelho A.A.: J. Appl. Crystallogr. *25*, 109 (1992).
37. Cheary R.W., Coelho A.A., Cline J.P.: Priority J. Res. Natl. Inst. Stand. Technol. *109*, 1 (2004).
38. Coelho A.A.: J. Appl. Crystallogr. *33*, 899-908 (2000).
39. Maki I.: in: Proceedings of the 8th International Congress of Cement Chemistry, p. 34-37, Rio de Janeiro, Brazil, 1986.
40. Liu X.C., Li Y.J.: Cem. Concr. Res. *35*, 1685 (2005).
41. Maki I., Fukuda K., Yoshida H., Kumaki J.: J. Am. Ceram. Soc. *75*, 3163 (1992).
42. Maki I., Goto K.: Cem. Concr. Res. *12*, 301 (1982).
43. Li X.R., Xu W.L., Wang S.P., Tang M.L., Shen X.D.: Cem. Concr. Res. *58*, 182 (2014).
44. Liu X.C., Li Y.J., Zhang N.: Cem. Concr. Res. *32*, 1125-1129 (2002).
45. Stanek T., Sulovsky P.: Cem. Concr. Res. *32*, 69 (2002).
46. Maki I., Fukuda K., Yoshida H., Kumaki J.: J. Am. Ceram. Soc. *75*, 3163 (1992).

47. Cuberos A.J.M., De la Torre A.G., Martín-Sedeño M.C., Moreno R.L., Merlini M., Ordonez L.M., Aranda M.A.G.: Cem. Concr. Res. *39*, 833 (2009).
48. Wang Q.Q., Li F., Shen X.D., Shi W.J., Li X.R., Guo Y.H., Xiong S.J., Zhuang Q.: Cem. Concr. Res. *57*, 28 (2014).
49. Bensted J.: Cem. Concr. Res. *8*, 73 (1978).
50. Campbell D.H.: *Microscopical Examination and Interpretation of Portland Cement and Clinker*, 2nd ed., p.16-18, 68-72, Portland Cement Association, the United States of America, 1999.
51. Wang H.: *Synthesis of belite-barium calcium sulphoaluminate via low grade raw materials*, M.S. Thesis, University of Jinan, 2010.
52. Wu H.X., Lu L.C., Yuan W.H., Cheng X.: Cem. Guid. New Epoch 5, 24 (2009).
53. Wu H.X., Lu L.C., Xuan H.Z., Cheng X.: J. Chin. Ceram. Soc. *22*, 226 (2008).